

## INFLUENCE OF VELOCITY GRADIENT ON OPTIMISATION OF THE AGGREGATION PROCESS AND PROPERTIES OF FORMED AGGREGATES

Part 2. Quantification of the influence of agitation intensity and time on the properties of formed aggregates

PAVEL POLÁŠEK

Institute of Hydrodynamics, AS CR, v.v.i., Pod Patankou 5, 166 12 Prague 6, Czech Republic; Mailto: polasek@ih.cas.cz

The follow up research into the IHDS process was carried out with a Couette device. The outcome of this study provides a comprehensive understanding of the effect that both the agitation intensity and the agitation time have on the kinetics and the mechanism of the aggregation process. The results obtained confirm the very favourable influence of high agitation intensity for the formation of more compact and dense aggregates than those formed by the accustomed flocculation conditions with low agitation intensity. This research also proved that the agitation intensity and time are the inherent means profoundly influencing the properties of the resultant aggregates such as their size, shape, density and homogeneity. Further, it was confirmed that the aggregation process passes through a minimum. Furthermore, it was verified that the aggregation process takes place in four consecutive phases, namely a) the phase of formation, b) the phase of compaction, c) the phase of a steady (equilibrium) state and d) most probably the phase of inner restructuring. The pattern of the aggregates development in these phases remains the same irrespective of the magnitude of the velocity gradient applied but the time at which these phases are completed is velocity gradient dependent. Last but not least this study proved that the dimensionless product  $Ca = \overline{G} T = \text{const.}$  has no general validity.

**KEY WORDS:** Inline High Density Suspension (IHDS) Formation Process, Aggregation Phases, Aggregate properties, Compactness, Relative Density of Aggregates.

Pavel Polášek: VLIV RYCHLOSTNÍHO GRADIENTU NA OPTIMALIZACI AGREGAČNÍHO PROCESU A VLASTNOSTI VYTVOŘENÝCH AGREGÁTŮ. Část 2. Kvantifikace vlivu rychlostního gradientu a času na vlastnosti vytvořených agregátů. J. Hydrol. Hydromech., 59, 2011, 3; 14 lit., 5 obr., 2 tab.

Výzkum tvorby agregátů metodou IHDS pokračoval s Couettovým typem flokulačního zařízení. Výsledek této studie umožňuje porozumět vlivu intenzity a času míchání na kinetiku a mechanismus agregačního procesu. Získané výsledky potvrzují velmi příznivý vliv vysoké intenzity míchání na tvorbu kompaktnějších a hustších agregátů než jsou ty vytvořené běžnými flokulačními podmínkami s nízkou intenzitou míchání. Tento výzkum také potvrdil, že intenzita míchání ve spojení s časem je přirozeným prostředkem výrazně ovlivňujícím vlastnosti výsledných agregátů jako je jejich rozměr, tvar, hustota a homogenost. Dále bylo potvrzeno, že agregační proces probíhá ve čtyřech následných fázích. Jedná se o: a) fázi tvorby, b) fázi zhutňování, c) fázi rovnovážného stavu a d) s největší pravděpodobností fázi vnitřní restrukturalizace. Struktura agregátů vytvořených v jednotlivých fázích je obdobná bez ohledu na velikost použitého rychlostního gradientu, ale čas potřebný k ukončení těchto fází je závislý na velikosti použitého rychlostního gradientu. V neposlední řadě tato studie potvrdila, že bezrozměrné kritérium  $Ca = \overline{G} T = \text{konst.}$  nemá všeobecnou platnost.

**KLÍČOVÁ SLOVA:** průtoková tvorba vysoko hustotní suspenze, IHDS metoda, fáze agregačního procesu, vlastnosti agregátů, kompaktnost, relativní hustota agregátů.

### 1. Introduction

The research into the quantification of the effect of agitation intensity and time on the morphological

and physical properties of flocculent aggregates was carried out in a Couette type flocculation device (Fig. 9). The Couette device is characterised by a thin layer (annular space) of water, where the

formation of aggregates takes place. It produces a relatively uniform distribution of the velocity field throughout the volume of agitated water and therefore also a fairly uniform distribution of velocity gradient throughout the entire volume of agitated water. The thin annular space enables the recording of the development of aggregates by photography. The use of the Couette device permits to study the trend of changes in the development of aggregates as they take place and which are hidden when jar tests are carried out in beakers.

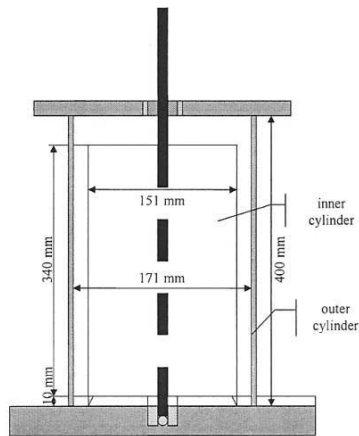


Fig. 9. The arrangement of Couette device.

There is a major difference between the character of flow in a Couette device and in beakers. In the Couette device a fairly uniform distribution of the velocity field exists even under modest turbulent conditions. In contrast, agitation in beakers creates a fully mixed system with a fluctuating agitation intensity having the highest intensity in the stirrer-tip zone and the lowest in the most remote places of the stirrer-bulk zone. Therefore, the aggregates being formed in the beakers are subjected to continuously changing velocity gradients as well as orientation of aggregates in the flow of water, irrespective of the stirrer speed. As a result, the resultant aggregates are likely to be more spherical and have different propensity to breakage than the aggregates formed under the flow conditions in the Couette device. It can be presupposed therefore, that the properties of the aggregates formed in the Couette device and in beakers differ in their absolute values. Nevertheless, the results obtained from the Couette device are very interesting and important because they illustrate the trend in the development of aggregates and the dependence of their properties on different intensities and times of agitation.

It is well known that during aggregation, the destabilised particles of impurities are combined into spatial structures forming the aggregates. In these structures there are large volumes of lattice spaces that are filled with trapped water. It stands to reason that volume of these lattice spaces is responsible for low density of aggregates (Tesarik, 1968; Hereit et al., 1980).

The structural configuration (compactness), size and density of the formed aggregates are influenced by the magnitudes of adhesive forces and tangential forces.

Whilst the adhesive forces are determined by the nature of impurities and the chemistry of the purification process the tangential forces are determined by the magnitude of velocity gradient  $\bar{G}$ .

The ratio of these forces influences the arrangement of the destabilised particles of impurities in an aggregate and hence its physical properties. The significance of the ratio of these forces on the structure of the formed aggregates can be described in agreement with Benze (1967a, 1967b, 1968) as follows: When the adhesive forces are incomparably greater than the tangential forces (low  $\bar{G}$ ), the combining particles/aggregates join each other at the point of contact. As a result, large and voluminous aggregates of anisometric shape and geometrically loose, widely branched, spatially extended net structure are formed. The ultimate aggregates are large, containing large volumes of voids (great porosity) that are filled with entrapped water. They are of low density and very fragile with a tendency to fragment.

In contrast, when the ratio of adhesive and tangential forces is low (high  $\bar{G}$ ), the combining particles/aggregates slide along each other until they occupy geometrically the most favourable and energetically the most stable position with respect to the existing agitation intensity. Therefore, when aggregates are formed with high  $\bar{G}$  they are of a smaller size and of more compact and thoroughly aligned inner structure. They are also more resistant to fragmentation. Such aggregates would have a smaller volume of voids (small porosity) and hence contain a smaller quantity of entrapped water. Therefore, their density should be higher.

When the tangential forces are considerably greater than the adhesive forces, the aggregation of particles does not occur.

There is an analogy between the deposition of the destabilised particles in aggregates and the nature of packing of sand grains in a filter bed. Both

are characterised by porosity, which varies with the nature of the packing in case of a sand bed, and the ratio between adhesive and tangential forces as well as the velocity gradient  $\bar{G}$  and its duration  $T$  in case of flocculent aggregates. Assuming the filter bed consists of spherical grains of the same diameter, *Deb* (1965) described the dependence of porosity of filter bed on the nature of its packing as follows. The tangent planes of the spherical grains at the points of their contact form multi-hedrons. The most loose deposition of the spheres exists when the multi-hedron is a cube, where the number of contacts is 6 and the porosity of this packing is  $\omega_p = 0.476$ . At the tightest deposition of these spheres, the tangent planes form a dodecahedron, where the number of contacts is 12 and the porosity of this packing is  $\omega_p = 0.2599$ .

Based on the mechanistic model of aggegation (*Hereit et al.*, 1980) it is assumed that the destabilised particles of impurities are spherical or almost spherical. Therefore, the above model can also be applied to the deposition of the destabilised particles in aggregates. The compactness of the arrangement of the deposited particles in an aggregate, i.e. its porosity, changes depending on how close the particles are to one another, and this is affected by  $\bar{G}$ . The aggregate porosity gradually decreases with increasing  $\bar{G}$  and  $T$ , as it transpires from Fig. 2 – Part 1 of this paper. Therefore, it can be reasonably deduced that the attainable porosity can be within the range of  $\omega_{MI} = 0.48 - 0.26$ , as determined by *Deb*, when the most compact micro-aggregates are formed by the IHDS process. Comparison of this micro-aggregate porosity with that attainable under the accustomed flocculation conditions (low agitation intensity),  $\omega_{MI} = 0.80 - 0.93$  (*Hereit et al.*, 1980), indicates the potential for densification of aggregates by the IHDS process. (*Mutl, Polasek, 2005; Polasek, Mutl, 2005b*).

Quantification of the effect of agitation intensity and time on the physical properties of aggregates formed is dealt with herein.

## 2. Experimental plant and methods

### 2.1 Arrangement of the Couette reactor

The Couette device used consists of a static outer barrel, I.D. = 171 mm x 400 mm height and a rotating inner barrel, O.D. = 151 mm x 340 mm height, driven by a variable speed drive. The agitated volume of water was 1.7 litres. This Couette device is shown in Fig. 9.

### 2.2 Velocity gradient

The particle collisions are affected by their drag velocity. The drag velocity increases with the increasing velocity differential between the neighbouring layers of water. This velocity differential across the layer of water is the instantaneous velocity gradient  $G$  in the flow. Since the velocity gradient changes across the profile of agitated water *Camp and Stein* (1943) substituted the instantaneous velocity gradient  $G$  by the root-mean-square velocity gradient  $\bar{G}$ . The root-mean-square velocity gradient  $\bar{G}$  is one of the basic design parameters used for the design of flocculation systems.

The instantaneous velocity gradient  $G$  was calculated according to *Van Duuren* (1968). The root-mean-square velocity gradient  $\bar{G}$  ( $\bar{G}^*$ ) was calculated from the torque measured as follows: The inner barrel of the Couette device was rotated at different RPM displayed on the drive. The outer barrel was pivoting on jewel bearings along its axis at top and bottom. A bending beam strain gauge measured the effect of the reaction force on the outer barrel resulting from the rotation of the inner barrel and transmitted via the water in the annular space. The resulting torque  $M$  is the product of the circumferential force and the radius of the outer barrel. The power input shaft to water and the velocity gradient  $\bar{G}$  were calculated according to the following equations

$$P_{SW} = \frac{RPM M}{9550} \quad [mW]$$

$$\bar{G} = \sqrt{\frac{P_{SW}}{V \mu}} \quad [s^{-1}]. \quad (1)$$

The conversion of RPM to both the instantaneous velocity gradient  $G$  and the root-mean-square velocity gradient  $\bar{G}$  is shown in Fig. 10. As is evident from this Fig. there is a considerable difference between the two. Therefore, the same value of  $G$  and  $\bar{G}$  does not reflect the same agitation intensity, the same distribution of the velocity field and hence are not mutually interchangeable.

### 2.3 Agitation time

The development of aggregates was monitored and pictures taken in the following agitation times:  $T = 0.5, 1, 3, 5, 7, 9, 12, 15, 20, 30, 45, 60, 90$  and 120 minutes.

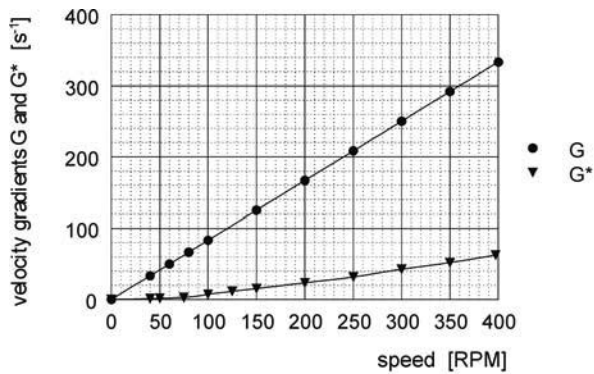


Fig. 10. Comparison of instantaneous velocity gradients  $G$  and root-mean-square velocity gradient  $G^*$  for the Couette flocculator.

#### 2.4 Raw water quality

For the reasons stated in Part 1 of this paper the jar tests were carried out with natural surface water from the impounding reservoir Vrchlice (Czech Republic). The quality of raw water used during testing is in Tab. 3.

Table 3. The quality of raw water used in the study.

Determinant	Units	Vrchlice dam
Temperature	[°C]	9.0 – 15.0
pH	[–]	8.4 – 9.1
Fe	[mg l <sup>-1</sup> ]	0.108 – 0.298
Total alkalinity	[mmol l <sup>-1</sup> ]	1.85 – 2.10
COD <sub>Mn</sub>	[mg O <sub>2</sub> l <sup>-1</sup> ]	5.05 – 5.60

#### 2.5 Destabilisation reagent used

Ferric sulphate was used as the destabilisation reagent. Its dosage was optimised by jar tests (Polasek and Mutl, 2005a). It was dosed into the Couette device evenly along its height when it was running at a speed at which the tests were carried out, and the completion of dosing was considered to be the commencement of the aggregation process, i.e.  $T = 0$ .

#### 2.6 Digital pictures and their processing

A photographic method developed by the UH-AVCR (Pivokonsky et al., 2002) and based on computer processing of pictures taken by a digital camera was used to evaluate the influence of different magnitudes of velocity gradients and different times of their action on the course of the formation of flocculent aggregates and their morphological

and physical properties. The development of aggregates was photographed with an Olympus Camedia 4040 digital camera at the agitation times stated in the foregoing. All images were taken to illustrate the development of aggregates at the same place of the Couette device. Digital images were taken using the TIFF format from the same area (2272 x 1704 pixels). Always only a narrow strip of a plane perpendicular to the camera lens where curvature of the Couette device is negligible was evaluated. Vertical dimension of the selected strip is the full dimension of the image and the horizontal dimension corresponds to 200 pixels. The size of the evaluated strip was always 200 x 1704 pixels and the resolution 0.04 mm.

After processing the digital images the number of formed aggregates was counted and the longitudinal dimensions in the direction of rotation and that perpendicular to it as well as the area of individual aggregates were measured and size-distribution of aggregates formed evaluated using SigmaScan software (Pivokonsky, 2002; Pivokonsky et al., 2004). In order to facilitate the processing of images a ruler in a millimetre scale was placed on the wall of the reactor and photographed with every image taken.

### 3. Result and discussion

The individual tests were carried out with the following velocity gradients  $\bar{G} = 1.3, 2.3, 3.8, 7.2, 15.6, 23.5, 31.9, 42.8, 52.0$  and  $62.7 \text{ s}^{-1}$ . The identification of aggregates formed with a  $\bar{G} \geq 23.5 \text{ s}^{-1}$  was difficult because the velocity of water was already high and the aggregates formed too small. Therefore, the margin of possible inaccuracy of the results obtained with a  $\bar{G} \geq 23.5 \text{ s}^{-1}$  increases with  $\bar{G}$ . Hence, the Couette device does not make it possible to test the effect of high  $\bar{G}$  that is used in the IHDS aggregation process and to investigate the impact of such high  $\bar{G}$  on the physical and rheological properties of aggregates formed.

#### 3.1 Influence of agitation intensity and its time on number of aggregates formed

Since aggregation is a time dependent process, the kinetics of this process is best described by changes in the number of aggregates in time. The development of aggregates characterised by the dependence of changes in the number of aggregates on different velocity gradients is illustrated in

Fig. 11. This Fig. shows that irrespective of  $\bar{G}$  applied the number of aggregates being formed drops to a minimum at the beginning of the aggregation process and then their number gradually increases until it evens out and a steady state of the aggregation process is reached. The period  $T_{min}$  required to reach the minimum number of aggregates being formed decreases with increasing agitation intensity ( $\bar{G}$ ). Furthermore, it is evident from this Fig. that the time of agitation required to reach a steady state is also  $\bar{G}$  dependent and the number

of aggregates formed in the steady state remains almost unchanged even over a prolonged agitation time.

The initial drop in the number of aggregates being formed at the very beginning of aggregation proves the extraordinary adhesive properties of the destabilised particles immediately after destabilisation. Most probably this is due to great adsorption capability produced by the hydroxocomplexes adhering to their surface.

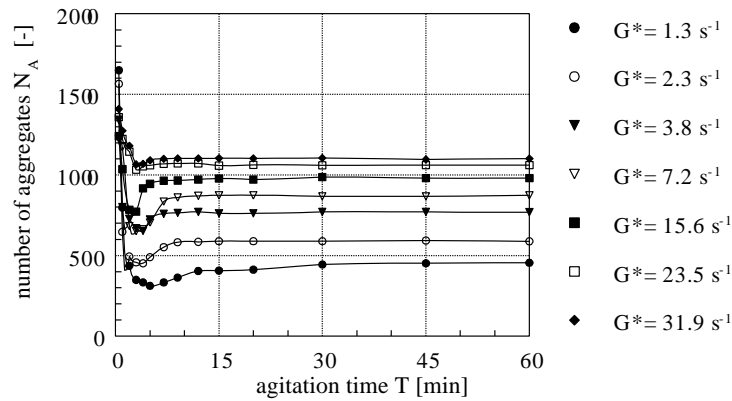


Fig. 11. Influence of intensity and duration of agitation on number of formed aggregates.

### 3.2 Dependence of size and shape of aggregates on agitation intensity and time

The conditions of agitation also affect the size and shape of the aggregates. The influence of agitation intensity and time on both of these parameters was evaluated from the measurements of longitudinal dimension  $l_1$  and  $l_2$  which is perpendicular to  $l_1$ , and the cross sectional area of aggregates  $F$ .

It follows from the dimensions measured that the aggregates formed in the Couette device are of a non-spherical shape. The shape circumscribed to an aggregate can be described as ellipsoid of rotation with the longer dimension being oriented in the direction of flow. With increasing agitation intensity the ratio of the ellipsoid longitudinal dimension  $l_1$  to  $l_2$  decreases as flow streamlining decreases and hence their ratio gradually balances.

The changes in aggregate sizes affect the changes in aggregate volume. For the UH-AVCR photographic method Pivokonsky (2002) proposed to calculate volume of the pictured aggregates as follows. From the measured dimensions  $l_1$  and  $l_2$ , it is possible to calculate the volume of an aggregate as the volume of a rotational body. This assumes that

the aggregates have the third dimension (depth) identical to the dimension  $l_2$ . The volume of a rotational ellipsoid is calculated according to the following formula:

$$V_A = V_{RE} = \frac{1}{6} \pi l_1 l_2^2. \quad (2)$$

Comparison of the dimensions of the horizontal and vertical axes enables the objective determination of the shape of formed aggregates. The closer their magnitudes are to one another the closer is their shape to a sphere. When all dimensions are the same the aggregates become spherical and their volume is calculated as follows:

$$V_A = V_S = \frac{1}{6} \pi d_A^3. \quad (3)$$

From the area of the pictured aggregate the diameter of a circle having the same area as that of the pictured aggregate is calculated as follows:

$$d_A = \sqrt{\frac{4F}{\pi}}. \quad (4)$$

This diameter can be used to calculate volume of the pictured aggregate  $V_A$  according to Eq. (3).

The effect of  $\bar{G}$  and  $T$  on the volume of formed aggregates is shown in Fig. 12. This Fig. shows that irrespective of  $\bar{G}$  applied the volume of aggregate  $V_A$  initially increases and after reaching a maximum it gradually decreases until a balanced volume is reached. The time required to attain the balanced volume is agitation intensity dependent – it de-

creases with increasing  $\bar{G}$  and corresponds to the time required to attain the steady state in terms of the number of aggregates formed. In the region of the steady state, the aggregate volume remains almost constant.

Furthermore, it follows from Fig. 12 that the maximum attainable aggregate size decreases with increasing  $\bar{G}$  and the homogeneity in size of the formed aggregates improves with aggregation time.

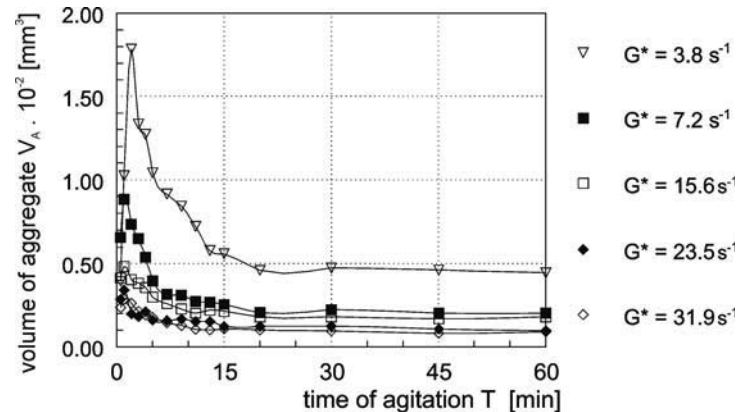


Fig. 12. Influence of intensity and time of agitation on volume of formed aggregates.

### 3.3 Model of development of aggregates

It follows from Figs. 11 and 12 that at the aggregation process passes through three consecutive phases. At the beginning of the aggregation process the combining of the destabilized particles into primary aggregates is facilitated by the extraordinary adhesive forces of the destabilised particles immediately after destabilisation. During this first phase, the phase of formation, the number of primary aggregates being formed decreases and their size (volume) increases. As soon as this extraordinary capacity of adhesive forces is exhausted the second phase, the phase of aggregate compaction, commences. During this second phase the number of aggregates being formed gradually increases and their size gradually decreases. As it is evident from Fig. 13, the compaction of aggregates takes place at the expense of the volume of voids aggregates. Consequently, compaction of aggregates increases concentration of the particles of impurities per unit volume of aggregates. The time required for the completion of the compactness of aggregates corresponds to the time needed to attain the steady state with respect to the number of formed aggregates.

When both the number and the size balance, the third phase, the phase of a steady state, is reached. During the phase of steady state both number and size of aggregates formed remains unchanged. Therefore, this third phase is considered to be the flocculation optimum.

A fourth phase of the aggregation process, the phase of inner restructuring/surface erosion, which follows from the results in Figs. 2 and 3 in Part 1 of this paper should also be included among the phases of aggregate development. This is because the reasons for reduced settleability of the aggregates formed under prolonged aggregation time could not be conclusively investigated as the results in Figs. 11 and 12 were obtained only with low velocity gradients.

The extent of changes between the individual phases corresponds to the velocity gradients applied. The minimum number of formed aggregates (Fig. 11) was found considerably lower than that formed at the steady state. Furthermore, a difference between the balanced number of aggregates formed at the steady state and the minimum number of formed aggregates increases with increasing  $\bar{G}$ . Similarly, the maximum volume of an aggregate

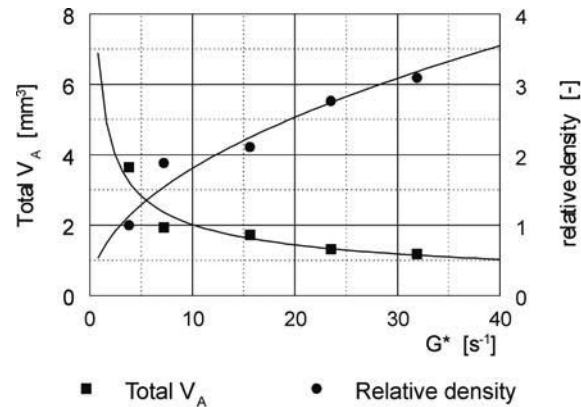


Fig. 13. Relative density of aggregates formed with different  $G^*$  at the flocculation optimum.

(Fig. 12) was found substantially greater than that of its balanced volume  $V_A$  reached at the steady state and a difference between maximum volume of an aggregate and its volume at the steady state decreases with increasing  $\bar{G}$ .

As already mentioned in the foregoing, the initial growth of aggregates to their maximum volume is the result of the greater initial adhesive force binding together the destabilised particles of impurities in the primary aggregates. The initial adhesive force is considerably greater than that of shear acting on the aggregates as result of the applied intensity of agitation ( $\bar{G}$ ). As the initial magnitude of the adhesive force gradually diminishes the aggregates being formed are unable to withstand the continuing influence of the agitation intensity ( $\bar{G}$ ) applied. This results in gradual breakage of these aggregates and their subsequent re-aggregation to the aggregates capable of withstanding the impact of shear produced by  $\bar{G}$  applied. The process of aggregate breakage is accompanied by the gradual increase in the number of aggregates being formed as is evident from Fig. 11. This restructuring process results in compaction of the aggregates. The compaction of aggregates takes place predominantly at the expense of the voids in aggregates which are filled with water. Consequently, compaction of aggregates increases concentration of the particles of impurities in the aggregates. The time required for the completion of the restructuring of aggregates corresponds to the time needed to attain the steady state with respect to the number of formed aggregates.

The pattern of the development of aggregates in these phases remains the same irrespective of the velocity gradient but the time at which the individ-

ual phases are completed is velocity gradient dependent.

The results in Figs 2 and 3 in Part 1 show decreasing settleability of aggregates formed with root-mean-square velocity gradient  $\bar{G} \gg 50 s^{-1}$  when their formation is completed well beyond the flocculation optimum. Although this aspect received considerable attention it could not be investigated indepth for the following reason. When aggregates were formed with a  $\bar{G} \leq 23.5 s^{-1}$  both number and dimensions of formed aggregates remained the same over prolonged aggregation time. When the photo-images were taken of the aggregates formed with  $\bar{G} \geq 31.9 s^{-1}$  they showed rather chaotically changing number of the aggregates being formed which results from the inaccuracy in identification and sizing of the aggregates being formed.

When agitation continues beyond the flocculation optimum, the tangential forces continue to affect the aggregates being formed by a few possible ways. The prolonged action of the tangential forces well beyond flocculation optimum may cause either bond fatigue resulting in fragmentation of aggregates or surface erosion of the formed aggregates. Should this be the case, the number of resultant aggregates will be increasing. The existence of either of the above could not be confirmed during these tests however as no increase in the number of primary and micro-aggregates was measured with the low  $\bar{G}$  applied during these tests. Another possibility is inner restructuring of the particles of impurities in aggregates. The prolonged action of the same tangential forces cannot affect the deposition of primary aggregates in the resultant aggregates. It can only do so through an

impact on the deposition of the particles of impurities in the primary aggregates which were formed during the perikinetic aggregation. This could produce a very gradual reduction in the size of the resultant aggregates. Such changes will manifest themselves only after a considerably prolonged agitation time, which is inversely proportional to  $\bar{G}$ . When aggregates were formed with a low  $\bar{G} \leq 31.9 \text{ s}^{-1}$  such changes were not noted within the longest agitation time applied.

Hence, the reason for decreasing the sedimentation velocity of aggregates formed with high  $\bar{G}$  during the agitation that prolonged well beyond the flocculation optimum remains inconclusive and further investigation into this aspect of aggregation is needed.

### 3.4 The effect of $\bar{G}$ and $T$ on density of formed aggregates

The aggregation process results in the formation of aggregates which are less dense than particles of impurities from which they are formed. Whilst the density of aggregates is low and approaches that of water, the aggregates formed are many times larger than the particles of impurities. Therefore, the sedimentation velocity of aggregates is higher than that of the particles of impurities. Obviously, the density of aggregates is dependent on the relative solids-water content in their structure.

The explanation regarding the significance of the agitation conditions on the inner aggregate structure, and thereby its density, can be found in the mechanism of aggregate formation. With high  $\bar{G}$  and low ratio of the adhesion and tangential forces the destabilised particles in the aggregates are shifting closer together until they occupy the closest position to one another at which they withstands the effect of tangential forces produced by the agitation intensity applied. Extension of the agitation time  $T$  beyond that of the flocculation optimum will not improve the resultant compactness of aggregates simply because the primary aggregates are already so close to one another that any prolonged agitation cannot bring them any closer to each other.

Tambo (1990) determined experimentally that the aggregate density is a function of the aggregate size. Even though this finding is valid in a broader sense, the foregoing shows that the aggregate density is primarily a function of hydrodynamic conditions under which aggregates are formed. This is because the hydrodynamic conditions determine the

ratio of adhesive and tangential forces, size of aggregates formed and also influences the total volume of voids in an aggregate as well as the number of the particles contained in an aggregate.

### 3.5 Relative density of aggregates

From the results in Figs. 3 and 4 it is possible to conceptualise the influence of  $\bar{G}$  and  $T$  on the density of formed aggregates. Since these tests were carried out with the same raw water, the same destabilisation reagent and its dosage, it may be assumed that the number of the destabilised particles of impurities and their mass were also the same for all the tests. What was changing with the changing  $\bar{G}$  and  $T$  is the number of aggregates formed in the phase of steady state of aggregation (Fig. 11), their size and total volume (Fig. 12). Furthermore, it is evident from Fig. 12 that the aggregates formed with the same  $\bar{G}$  at the phase of steady state are homogeneous in size. If the total mass of all particles of impurities in the system is the same and the total volume of all formed aggregates changes with different  $\bar{G}$ , then it stands to reason that with a smaller total volume of all aggregates their density has to be greater and vice versa.

Since the absolute value of the particle (aggregate) mass in the system is unknown it is not possible to determine the density of aggregates formed with different  $\bar{G}$ . However, it is possible to determine the relative density of formed aggregates in comparison to a reference system the aggregate density of which is considered to be unit ( $\rho_{AR} = 1.0$ ). In other words, it is possible to determine by how much the density of aggregates has changed by means of different  $\bar{G}$  in relation to the unit system.

When  $N_A$  is total number of aggregates formed and  $V_A$  is the volume of an aggregate then total volume of all aggregates becomes

$$\Sigma V_A = N_A V_A \quad (5)$$

The total mass of all aggregates formed in the system of the same water under the optimised reaction conditions is the same irrespective of the velocity gradient  $\bar{G}$

$$M_G = M_{Gn} = \text{const.} \quad (6)$$

$M_G$  is a mass of aggregates formed at the flocculation optimum of the system and it is calculated according to the equation

$$M_G = \Sigma V_A \rho_A. \quad (7)$$

When the reference total volume of aggregates formed  $\Sigma V_R = \Sigma V_A$  to which comparison is made then its aggregate density  $\rho_G$  is also the reference density and  $\rho_R = \rho_A = 1$  and Eq. (6) can be modified as follows

$$\frac{\Sigma V_A \rho_A}{\Sigma V_R \rho_R} = \frac{M_G}{M_R} = 1. \quad (8)$$

When aggregates are formed with a different velocity gradient  $\bar{G}_n$  their total volume  $\Sigma V_{Gn}$  and density  $\rho_{Gn}$  changes. Ratio of the total volume of all aggregates  $\Sigma V_{Gn}$  formed with a different velocity gradient  $\bar{G}_n$  to the reference total volume of aggregates  $\Sigma V_R$  determines the reference value  $R_{Gn}$  of the system for a particular velocity gradient  $\bar{G}_n$  applied

$$\frac{\Sigma V_{Gn}}{\Sigma V_R} = R_{Gn}. \quad (9)$$

The relative density  $\rho R_{Gn}$  of aggregates formed with a different velocity gradient  $\bar{G}_n$  then becomes

$$\rho R_{Gn} = \frac{\rho_R}{R_{Gn}} = \frac{1}{R_{Gn}}. \quad (10)$$

The relatively density  $\rho R_{Gn}$  of aggregates formed under the conditions of Fig. 3 and 4, reviewed in Tab. 4 and linked to the reference aggregates formed with  $\bar{G} = 3.8 \text{ s}^{-1}$ , is illustrated in Fig. 13.

As it is evident from Fig. 13 the total volume of all aggregates  $\Sigma V_G$  formed at the flocculation optimum decreases with increasing velocity gradient and the rate of such decrease gradually decrease-

with increasing velocity gradient. Furthermore, the relative density  $\rho R_{Gn}$  of the aggregates formed at the flocculation optimum is increasing with increasing velocity gradient and that the rate of this increase gradually decreases with increasing velocity gradients as more compact aggregates are formed.

It can be deduced from Fig. 13 that from a certain velocity gradient both the total volume of all aggregates  $\Sigma V_G$  as well as their relative density  $\rho R_{Gn}$  will remain constant because the particles in the aggregates will already be most tightly deposited so that they would not be able to change their position with any further increase in velocity gradient and time of its application.

The relative density  $\rho R_{Gn}$  of an aggregate formed with  $\bar{G} = 31.9 \text{ s}^{-1}$  was found to be about 3 times higher than that of an aggregate formed with  $\bar{G} = 3.8 \text{ s}^{-1}$ . This confirms agitation intensity is the inherent means influencing compactness of the inner structure and thereby the density of formed aggregates.

Furthermore, it is also evident from Fig. 13 that the relative density of the aggregates formed at the flocculation optimum is increasing with increasing velocity gradient. The rate of this increase gradually decreases with increasing velocity gradients as more compact aggregates are formed.

It can also be deduced from Fig. 13 that from a certain velocity gradient the density of the aggregates formed will remain constant because the particles in the micro-aggregates will already be deposited most tightly and the compactness of the aggregates formed cannot be improved with any further increase in velocity gradient and time of its application.

Table 4. The density of aggregates formed at the flocculation optimum with different  $\bar{G}_{HI}$  and compared to that of aggregates formed with reference  $\bar{G} = 3.8 \text{ s}^{-1}$  (based on data in Figs. 11 and 12).

$\bar{G}$ [s <sup>-1</sup> ]	Measured values			Calculated values	
	N <sub>A</sub> [-]	V <sub>A</sub> [mm <sup>3</sup> ]	ΣV <sub>Gn</sub> [mm <sup>3</sup> ]	R <sub>Gn</sub> [-]	ρR <sub>Gn</sub> [-]
3.8	770	0.00473436	3.645459	1.0	1.0
7.2	868	0.00222949	1.935196	0.530851	1.883767
15.6	964	0.00179420	1.727488	0.473874	2.110266
23.5	1063	0.00123991	1.318023	0.361552	2.765800
31.9	1103	0.00106828	1.178321	0.323230	3.093774

#### 4. Conclusions

1. The outcome of this study is understanding of the effect of velocity gradient and its duration on the

kinetics and the mechanisms of the aggregation process and the morphological and the physical properties of the resultant aggregates.

2. It was established that the process of formation of aggregates takes place in four consecutive phases following one another:
- the phase of formation,
  - the phase of compaction,
  - the phase of a steady (equilibrium) state,
  - the phase of inner restructuring – well beyond the flocculation optimum and applicable to agitation intensity characterised by  $\bar{G} \gg 50 \text{ s}^{-1}$ .

The pattern of development of aggregates in these phases remains the same irrespective of the velocity gradient but the time at which the individual phases are completed is velocity gradient dependent.

3. The condition of agitation under which aggregation takes place has a decisive effect on the structure and the physical properties of the resultant aggregates.
4. The high intensity agitation is the inherent means favourably affecting density of aggregates. The relative density of aggregates formed with  $\bar{G} = 31.9 \text{ s}^{-1}$  was found to be about 3 times higher than that of aggregates formed with  $\bar{G} = 3.8 \text{ s}^{-1}$ .

*Acknowledgement.* The research project has been funded by the Grant Agency of the Czech Republic under the project No. 103/07/1016 and Institutional Research Plan No. AV0Z20600510. The financial assistance on this project is acknowledged.

#### List of symbols

$d_A$	– diameter of spherical aggregate [m],
Ca	– Camp number [–],
$F$	– area of the pictured aggregate [ $\text{m}^2$ ],
$G$	– instantaneous velocity gradient [ $\text{s}^{-1}$ ],
$\bar{G}, G^*$	– mean-root-square velocity gradient [ $\text{s}^{-1}$ ],
I.D.	– inside diameter [m],
$l_1$	– longitudinal dimension of aggregate [m],
$l_2$	– dimension of aggregate perpendicular to $l_1$ [m],
$M$	– moment of force (torque) measured [mW],
$M_{Gn}$	– mass of aggregates formed with $\bar{G}_n$ ,
$M_R$	– mass of reference aggregates,
$M_G$	– mass of aggregates formed with a $\bar{G}$ [ $\text{kg m}^3$ ],
$N_A$	– number of aggregates [–],
O.D.	– outside diameter [m],
$P_{SW}$	– power input shaft to water [ $\text{kg m}^2 \text{ s}^{-3}$ ],
RPM	– the inner barrel revolutions per minute [ $\text{min}^{-1}$ ],
$T$	– time [s],
$V$	– volume of water [ $\text{m}^3$ ],
$V_A$	– volume of aggregate [ $\text{m}^3$ ],
$V_{RE}$	– volume of ellipsoid of rotation [ $\text{m}^3$ ],
$V_S$	– volume of sphere [ $\text{m}^3$ ],
$\Sigma V_R$	– total reference volume of aggregate,
$\Sigma V_A$	– total volume of all aggregates formed [ $\text{m}^3$ ],

$\Sigma V_G$	– total volume of all aggregates formed with a $\bar{G}$ , [ $\text{m}^3$ ],
$R$	– relative density of aggregate [–],
$R_{GN}$	– reference value for $\bar{G}_n$ ,
$\rho R_{GN}$	– relative density of aggregates formed with $\bar{G}_n$ ,
$\omega_{MI}$	– porosity of micro-aggregates [–],
$\rho_A$	– density of aggregates,
$\omega_P$	– porosity of filter media packing [–],
$\mu$	– viscosity of water [ $\text{kg m}^{-1} \text{ s}^{-1}$ ].

#### REFERENCES

- BENZE F., 1967a): Ein Beitrag zur Koagulationstheorie und zur Scherbeanspruchung von Abwasser Flocken. Dissertation TH Aachen.
- BENZE F., 1967b): Koagulation und Flockenfestigkeit in Scherströmungen. Chemie-Ing.- Technik, 39, 1116–1120.
- BENZE F., 1968: Untersuchungen über die Flockenfestigkeit in Scherströmungen. D-Monograph, 59, 1045–1069, Verlagchemie GmbH.
- CAMP T.R. and STEIN P.C., 1943: Velocity gradients and internal work in fluid motion. J. Boston Soc. Civ. Engrs., 4, 219–237.
- DEB A.K., 1965: Theory of Water Filtration – Discussion. J. San. Eng. Div., SA 1, 91–98.
- HEREIT F., MUTL S. and VAGNER V., 1980: The formation of separable suspensions and the methods of its assessment. J. Water Suppl.: Res Technol. AQUA, 29, 95–99.
- MUTL S. and POLASEK P., 2005: The influence of G and T on the properties of aggregates. Proc. IWA Specialised conference: Particle Separation 2005: Sustainable and Innovative Technologies to Meet MDGs, 1–3 June 2005, Seoul, Korea.
- PIVOKONSKY M., 2002: Influence of the velocity gradient and time of its application on the size characteristic of the aggregates formed during agitation (in Czech). Ph.D. Thesis, Faculty of Sciences, Institute for Environmental Studies, Charles University, Prague, Czech Republic.
- PIVOKONSKY M., PIVOKONSKY R., BENESOVA L. and MUTL S., 2004: Methodology of evaluation of size and size-distribution of particles formed during aggregation. J. Hydrol. Hydromech., 51, 4, 281–287.
- POLASEK P. and MUTL S., 2005a): Optimisation of reaction conditions of particles aggregation in water purification. Water SA, 28, 1, 61–72.
- POLASEK P. and MUTL S., 2005b): High rate clarification technology. Proc. IWA Specialised conference: Particle Separation 2005: Sustainable and Innovative Technologies to Meet MDGs, 1–3 June 2005, Seoul, Korea.
- TAMBO N., 1990: Basic concept and innovative turn of coagulation/flocculation. Proc. Jonkoping, Water Supply, 8, 1–10.
- TESARIK I., 1968: Discussion to: Ives K: Theory of operation of sludge blanket clarifiers. Proc. Instn. Civ. Engrs, 39, p. 569.
- VAN DUUREN F.A., 1968: Defined velocity gradient model flocculator. J. San. Eng. Div., SA 4, 671–682.

Received 17 March 2010  
Accepted 26 October 2010